Electronic Supplementary Information (ESI) for

A triphasic nanocomposites with synergetic interfacial structure as efficient trifunctional electrocatalysts for electrochemical oxygen and hydrogen reactions

Ying Wang*, Hongjie Yuan, Fan Liu, Tianjun Hu†

Key Laboratory of Magnetic Molecules & Magnetic Information Materials Ministry of Education, The School of Chemical and Material Science, Shanxi Normal University, Linfen 041004, China.

* Corresponding author. E-mail address: wangyinghc@sxnu.edu.cn (Y. Wang)
† Corresponding author. E-mail address: hutj@sxnu.edu.cn (T. Hu)

Physical Characterization

The crystal structure of samples was tested by X-ray diffraction (XRD) using Rigaku ultima IV diffractometer. The morphology was characterized by Scanning electron microscopy (SEM) using JFC1600 microscope. Transmission electron microscopy (TEM) and high-resolution transmission electron microscopy (HRTEM) characterization was completed by using JEM-2100 instrument. The valence states of chemical elements were charactered by X-ray photoelectron spectroscopy (XPS) using VG ESCALAB 210 instrument. The compositions of the products were examined by inductively coupled plasma-optical emission spectrometry (ICP-OES, X Series 2, Thermo Scientific USA).

Electrochemical Measurements

The catalytic activity was performed on a CHI 660E electrochemical workstation with a standard three-electrode system, where Hg/HgO and Pt wire (OER) or graphite rod (HER) used as the reference electrode and counter electrode, respectively. The rotating disk electrode (0.126 cm^2) with catalysts loading of 0.2 mg cm^{-2} was used as the working electrode. The ORR and OER tests were carried out in O_2-saturated 0.1 M KOH solution with sweep rate of 10 mV s^{-1}. The HER measurements were performed in N_2-saturated 1 M KOH solution with a scan rate of 5 mV s^{-1}. The Nyquist plots were measured in a frequency range from 100 kHz to 0.1 Hz with potential amplitude of 5 mV. The electrochemically active surface area (ECSA) can be evaluated by the double-layer capacitance (C_{dl}) which is determined via cyclic voltanmmetry (CV) method.

The rechargeable Zn-air batteries were tested in 6 M KOH with home-made electrochemical cell. A polished Zn plate and a carbon paper coated with the prepared catalyst ink (1 mg cm^{-2}) were used as the anode and air cathode, respectively. The conventional Pt/C + RuO_2 mixture catalyst with 1:1 mass ratio was prepared with the same mass loading.

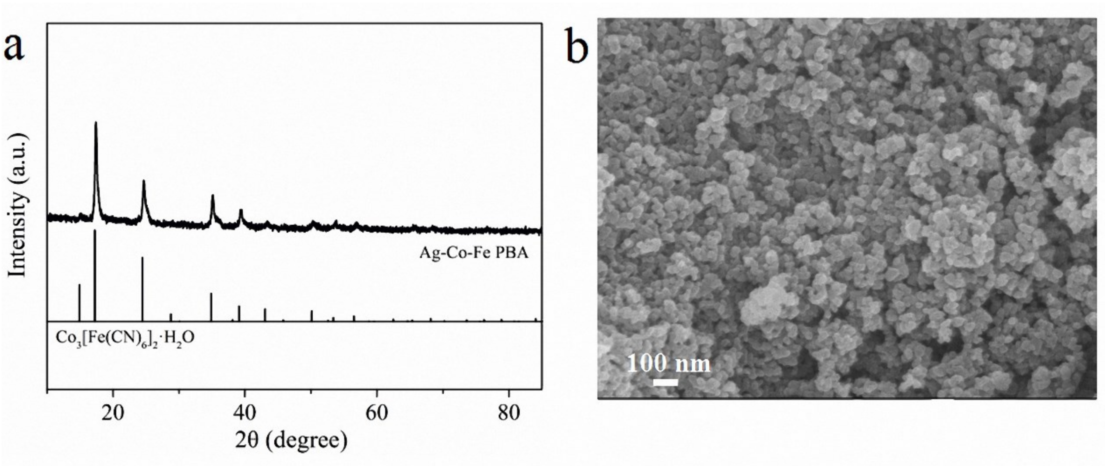

Fig. S1 (a) The XRD pattern of Ag-Co-Fe-PBA; (b) SEM image of Ag-Co-Fe-PBA.

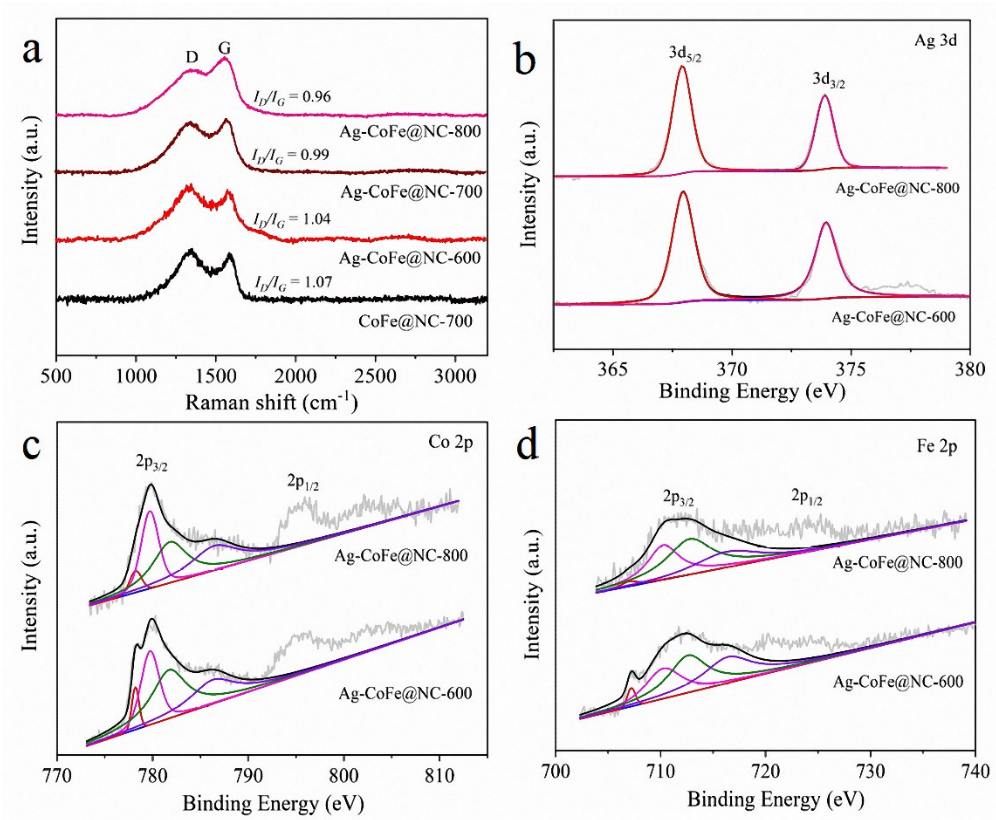

Fig. S2 (a) Raman spectra of samples; (b-d) XPS spectra of Ag 3d, Co 2p and Fe 2p of Ag-CoFe@NC-600 and Ag-CoFe@NC-800.

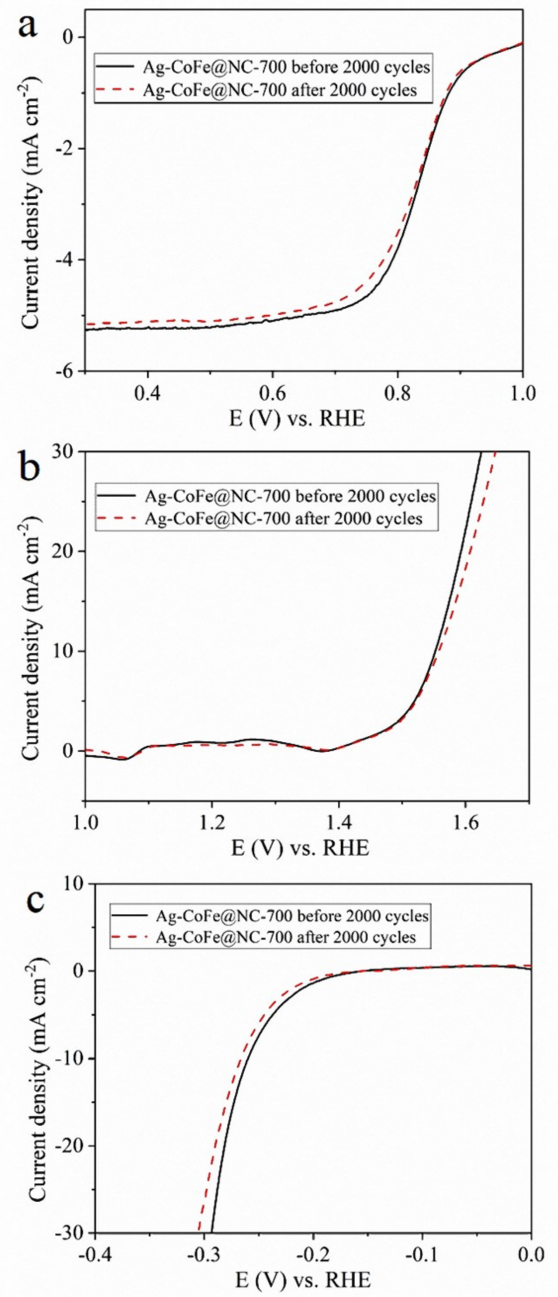

Fig. S3 LSV curves of Ag-CoFe@NC-700 for ORR (a), OER (b) and HER (c) before and after 2000 cycles.

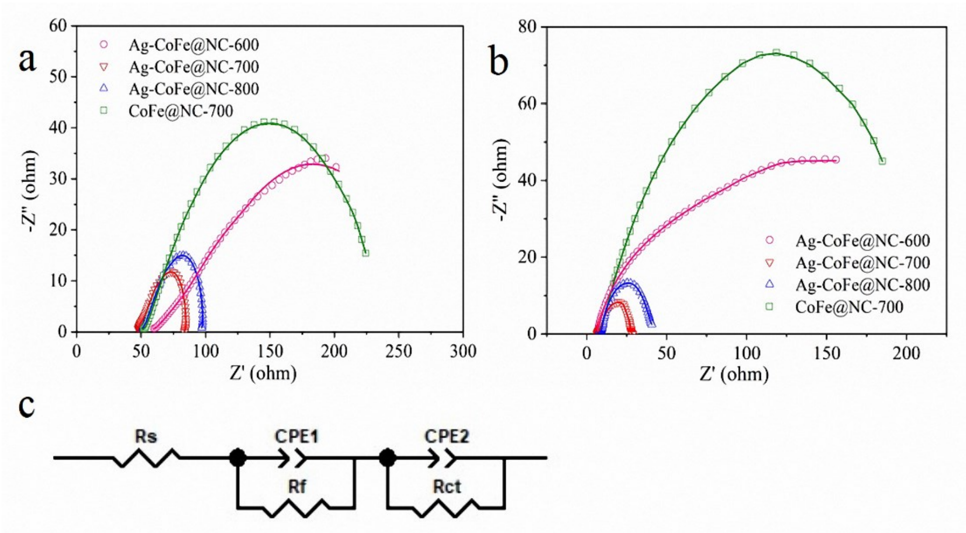

Fig. S4 (a) Nyquist plots of Ag-CoFe@NC samples obtained from EIS measurements at the potential of 1.55 V for OER; (b) Nyquist plots of Ag-CoFe@NC samples obtained from EIS measurements at the potential of -0.26 V for HER; (c) Equivalent electrical circuit used to model OER and HER kinetics process, where R_s is the solution resistance. R_f is the resistance associated to the GCE/catalyst interface, and R_{ct} is the charge transfer resistance at catalyst/electrolyte interface.

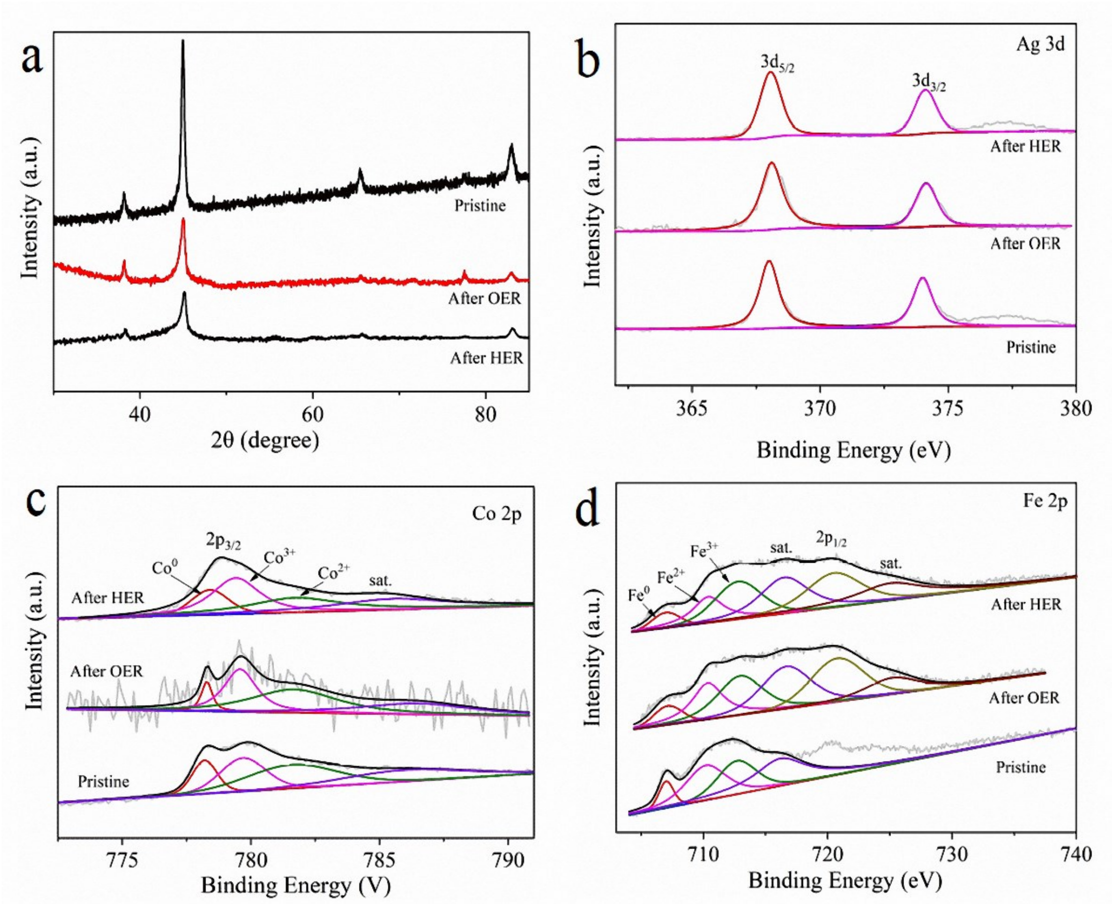

Fig. S5 (a) The XRD patterns of Ag-CoFe@NC-700 before and after stability test; (b)-(d) XPS spectra of Ag 3d, Co 2p and Fe 2p for Ag-CoFe@NC-700 before and after stability test.

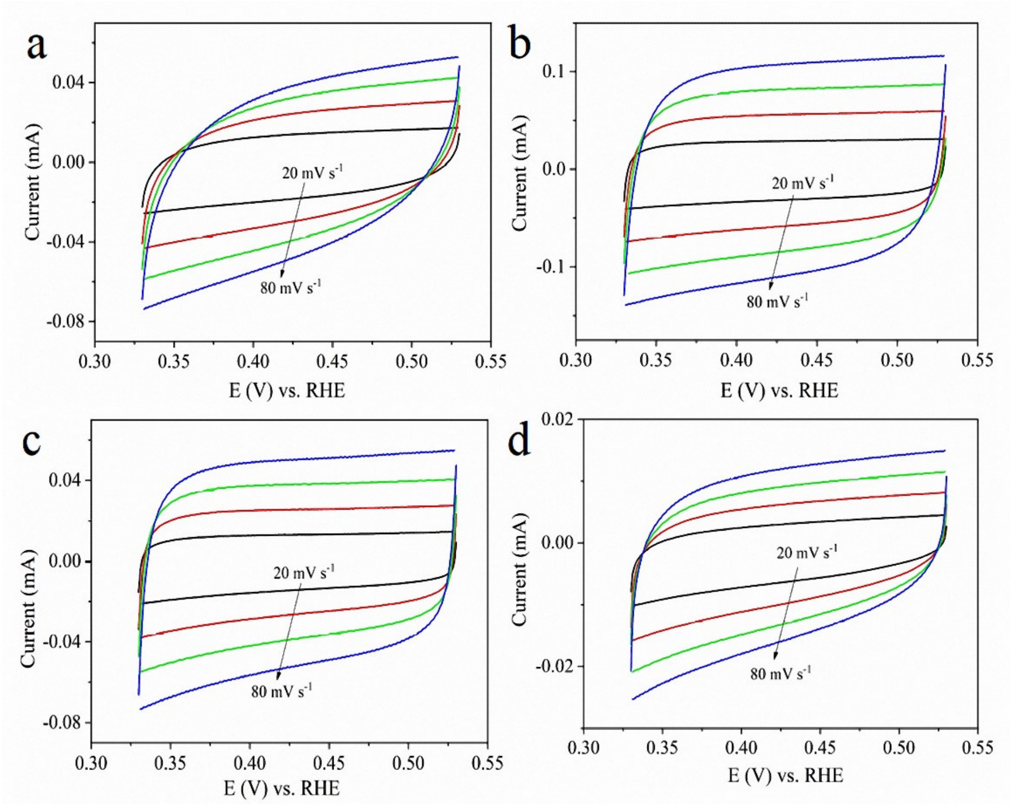

Fig. S6 CV curves at different scan rates for Ag-CoFe@NC-600 (a), Ag-CoFe@NC-700 (b), Ag-CoFe@NC-800 (c) and CoFe@NC-700 (d).

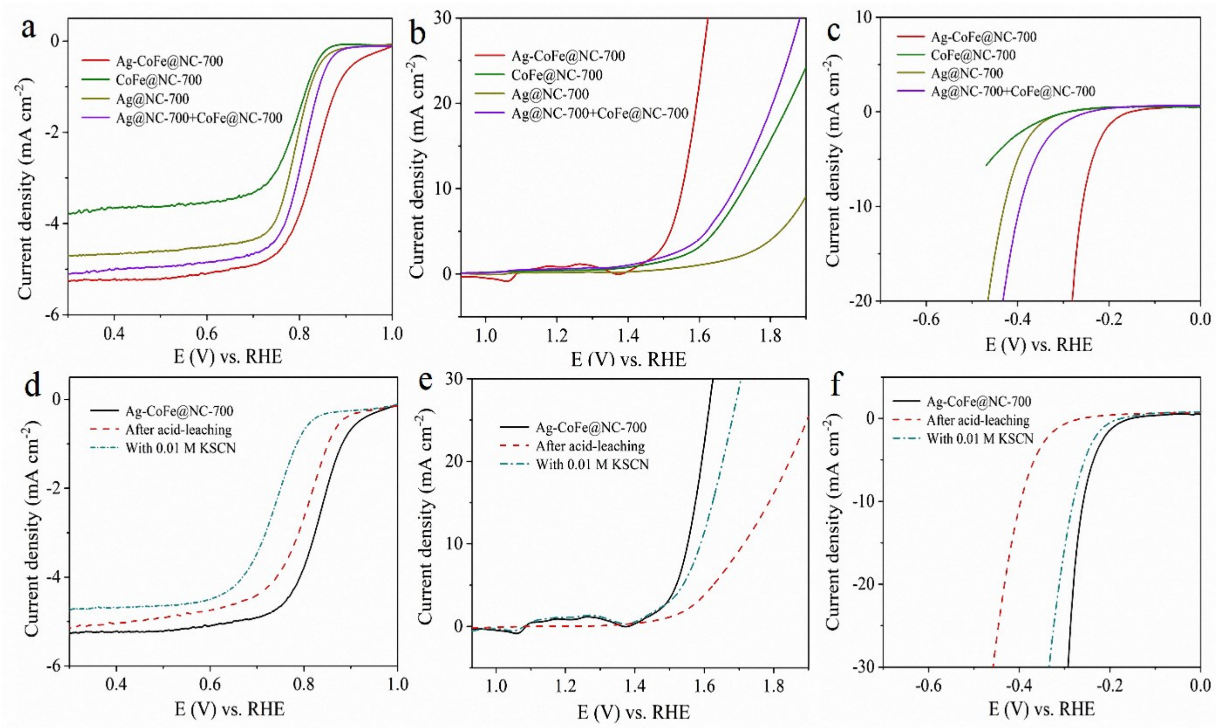

Fig. S7 LSV curves of Ag-CoFe@NC-700, CoFe@NC-700, Ag@NC-700 and Ag@NC-700+CoFe@NC-700 (1:7.4) for ORR (a), OER (b) and HER (c); LSV curves for ORR (d), OER (e) and HER (f) before and after acid-leaching and poisoning treatment with 0.01 KSCN in electrolyte.

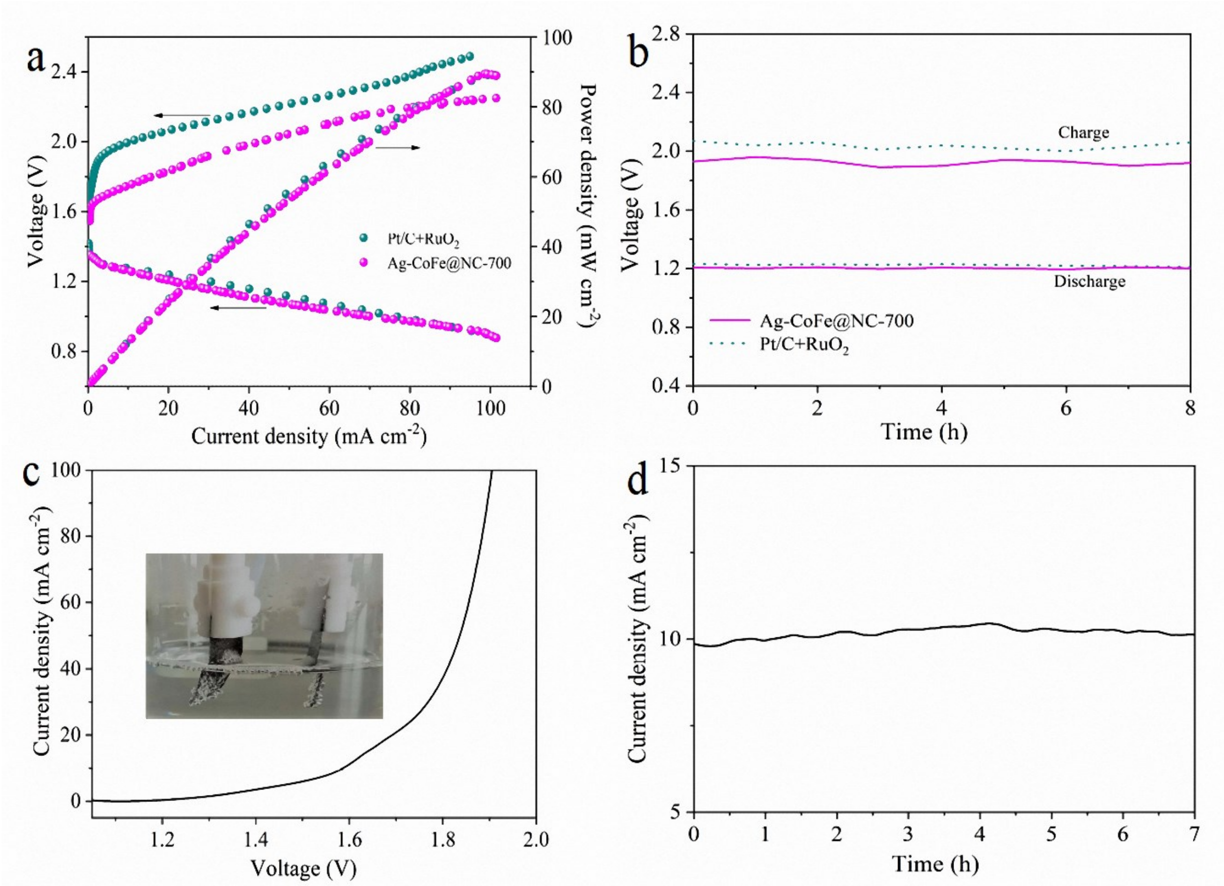

Fig. S8 (a) Charge and discharge polarization curves and the power densities of zinc-air battery via using Ag-CoFe@NC-700 and Pt/C + RuO_2 as the air catalysts, repectively; (b) Long-time galvanostatic discharge and charge curves at 20 mA cm^{-2}; (c) LSV curves of water electrolysis based on Ag-CoFe@NC-700 in 1 M KOH. The inset shows the photogtaph of the generation of hydrogen and oxygen bubbles on electrode; (d) The durability test at 10 mA cm^{-2}.

Tabel S1 The surface chemical compositions of catalyst obtained by XPS.

Sample	C (at.%)	O (at.%)	Ag (at.%)	Co (at.%)	Fe (at.%)	N (at.%)
Ag-CoFe@NC-600	80.78	11.85	0.52	1.51	1.45	3.89
Ag-CoFe@NC-700	82.10	9.48	0.71	2.13	2.06	3.52
Ag-CoFe@NC-800	84.92	8.29	0.62	1.92	1.82	2.43
CoFe@NC-700	79.28	16.24	-	1.14	1.09	2.25

Tabel S2 N 1s components of samples collected from XPS results.

Sample	Total N content (at.%)	Relative peak area percentage (%) [a]				
		N1	N2	N3	N4	N5
Ag-CoFe@NC-600	3.89	27.51	6.13	45.53	9.12	11.71
Ag-CoFe@NC-700	3.52	32.17	6.65	32.54	17.42	11.22
Ag-CoFe@NC-800	2.43	1.93	1.84	21.33	53.96	20.94
CoFe@NC-700	2.25	11.42	2.41	70.55	15.62	-

[a] N1: pyridinic N; N2: M-N; N3: pyrrolic N; N4: graphitic N; N5: oxidized N.

Table S3 The chemical composition obtained by ICP-OES.

Sample	Ag (wt.%)	Co (wt.%)	Fe (wt.%)
Ag-CoFe@NC-600	1.61	4.38	4.49
Ag-CoFe@NC-700	2.20	6.39	5.97
Ag-CoFe@NC-800	1.90	5.86	5.42
CoFe@NC-700	-	3.42	3.38
Ag@NC-700	8.78	-	-

Table S4 Comparison in the oxygen electrode activities

Catalyst material	$E_{j=1/2}$ (V)	$E_{j=10}$ (V)	ΔE (V)	Reference
Ag-CoFe@NC-700	0.83	1.55	0.72	This work
Co-Co3O4@NAC	0.80	1.61	0.81	[1]
HHPC	0.78	1.58	0.80	[2]
Co@CNT/MSC	0.84	1.62	0.78	[3]
FeCo@NCNS	0.83	1.60	0.77	[4]
FeCo-NCNFs-800	0.82	1.69	0.87	[5]
Ni_3Fe/N-C sheets	0.78	1.62	0.84	[6]
FeCo/FeCoNi@NCNTs-HF	0.85	1.61	0.76	[7]
FeNiCo@NC-P	0.84	1.54	0.70	[8]
DAP-DAB-$C_4H_6O_4$·Co·$4H_2O$	0.88	1.60	0.72	[9]
H-Co@FeCo/N/C	0.91	1.61	0.70	[10]
C-MOF-C2-900	0.82	1.58	0.76	[11]
3C-900	0.82 ($E_{j=-3}$)	1.60	0.78	[12]
NiCo-0.8@N-CNFs-800	0.82	1.61	0.79	[13]
Co@Co_3O_4/N-C	0.81	1.62	0.81	[14]
FeNi/N-CPCF-950	0.87	1.59	0.72	[15]
Co_9S_8-NSHPCNF	0.82	1.58	0.76	[16]

References

[1] X. Zhong, W. Yi, Y. Qu, L. Zhang, H. Bai, Y. Zhu, J. Wan, S. Chen, M. Yang, L. Huang, M. Gu, H. Pan, B. Xu, Appl. Catal. B, Environ. 260 (2020) 118188.

[2] X. Xiao, X. Li, Z. Wang, G. Yan, H. Guo, Q. Hu, L. Li, Y. Liu, J. Wang, Appl. Catal. B, Environ. 265 (2020) 118603.

[3] C. Xiao, J. Luo, M. Tan, Y. Xiao, B. Gao, Y. Zheng, B. Lin, J. Power Sources 453 (2020) 227900.

[4] T. Liu, S. Cai, Z. Gao, S. Liu, H. Li, L. Chen, M. Li, H. Guo, Electrochim. Acta 335 (2020) 135647.

[5] L. Yang, S. Feng, G. Xu, B. Wei, L. Zhang, ACS Sustain. Chem. Eng. 7 (2019)

5462-5475.
[6] G. Fu, Z. Cui, Y. Chen, Y. Li, Y. Tang, J.B. Goodenough, Adv. Energy Mater. 7 (2017) 1601172.
[7] Z. Wang, J. Ang, B. Zhang, Y. Zhang, X.Y.D. Ma, T. Yan, J. Liu, B. Che, Y. Huang, X. Lu, Appl. Catal. B, Environ. 254 (2019) 26-36.
[8] D. Ren, J. Ying, M. Xiao, Y.P. Deng, J. Ou, J. Zhu, G. Liu, Y. Pei, S. Li, A.M. Jauhar, H. Jin, S. Wang, D. Su, A. Yu, Z. Chen, Adv. Funct. Mater. 30 (2019) 1908167.
[9] D. Lyu, Y. Du, S. Huang, B.Y. Mollamahale, X. Zhang, S.W. Hasan, F. Yu, S. Wang, Z.Q. Tian, P.K. Shen, ACS Appl Mater Interfaces 11 (2019) 39809-39819.
[10] Y.-j. Wu, X.-h. Wu, T.-x. Tu, P.-f. Zhang, J.-t. Li, Y. Zhou, L. Huang, S.-g. Sun, Appl. Catal. B, Environ. 278 (2020) 119259.
[11] M. Zhang, Q. Dai, H. Zheng, M. Chen, L. Dai, Adv. Mater. 30 (2018) 1705431.
[12] T. Li, Y. Lu, S. Zhao, Z.-D. Gao, Y.-Y. Song, J. Mater. Chem. A 6 (2018) 3730-3737.
[13] C. Feng, Y. Guo, Y. Xie, X. Cao, S. Li, L. Zhang, W. Wang, J. Wang, Nanoscale 12 (2020) 5942-5952.
[14] Y. Wang, T. Hu, Y. Qiao, Y. Chen, L. Zhang, Chem. Commun. 54 (2018) 12746-12749.
[15] Z. Wang, J. Ang, J. Liu, X.Y.D. Ma, J. Kong, Y. Zhang, T. Yan, X. Lu, Appl. Catal. B, Environ. 263 (2020) 118344.
[16] W. Peng, Y. Wang, X. Yang, L. Mao, J. Jin, S. Yang, K. Fu, G. Li, Appl. Catal. B, Environ. 268 (2020) 118437.